Penerbit UTHM

PAAT

http://publisher.uthm.edu.my/ojs/index.php/paat

e-ISSN : 2821-2924

Progress in Aerospace and Aviation Technology

Development of Obstacle Detection System Based On the Integration of Different Based Sensor for Small-Sized UAV

Muhammad Amirul Nawawi[1], Muhammad Faiz Ramli[2]*

[1]Faculty Mechanical and Manufacturing Engineering,
Universiti Tun Hussein Onn Malaysia (UTHM), Batu Pahat, 86400, MALAYSIA

[2]Aircraft System and Design Research, Faculty Mechanical and Manufacturing Engineering,
Universiti Tun Hussein Onn Malaysia (UTHM), Batu Pahat, 86400, MALAYSIA

*Corresponding Author

DOI: https://doi.org/10.30880/paat.2023.03.01.003
Received 21 February 2023; Accepted 19 June 2023; Available online 31 July 2023

Abstract: Due to the physical size and weight limits of small unmanned aerial vehicles (UAVs), developing a reliable obstacle detection a system that can provide an effective and safe avoidance path is extremely difficult. Prior work has tended to use a vision-based sensor as the primary detecting sensor however, this has resulted in a high reliance on texture appearance and a lack of distance sensing capabilities. Furthermore, due to the inability to detect the free region, vision-based sensor detection systems have difficulty developing a trusted safe avoidance path. However, most wide spectrum range sensors are bulky and expensive, making them unsuitable for small UAVs. This project aims to construct an obstacles detection system with the integration of various based sensors for a small UAV. The potential obstacles are identified by categorizing feature points identified in image frame. The suggested approach was tested in a real-world setting for both of the observed scenarios, which included various obstacles configurations. Two types of scenarios are experimented in this project consists of single frontal obstacles and presence of side obstacles alongside the frontal obstacles. On top of that, the position of the side obstacle is aligned to the frontal obstacle and then will be positioned in the increment of 20cm further from the frontal obstacle in order to analyze the outcome of the proposed algorithm. The proposed detection system had a possibility to be a trustworthy system even after utilizing the depth perception technique, however this does not imply that the proposed system is faultless. The results show that the suggested algorithm system detects and distinguishes between the potential obstacles and free region for a single frontal obstacle perfectly. However, there were improvements that should be implemented with the proposed system's ability of detection for multiple obstacles.

Keywords: OpenCV, UAV, LiDAR, Raspberry Pi

1. Introduction

In recent years, the civilian application of unmanned aerial vehicles (UAVs) has grown dramatically, and it is no longer limited to the military context. UAV stands for unmanned aerial vehicle, and it is a motorised air aircraft that does not require an onboard pilot. It can fly autonomously or with manual control from a human pilot on the ground thanks to the embedded system of the UAV being pre-programmed. The obstacle detection system is regarded as an important element in the autonomous navigation system [1][2]. It allows the UAV to carry out its job in a safe manner across the operational area [3]–[7]. However, there are many deficiencies in this study that need to be filled because most previous obstacle detection and systems established by researchers still have flaws and drawbacks that can compromise the system's resilience and reliability. This project aims to address all of the aforementioned flaws and issues by introducing a novel obstacle detection system based on a vision-based sensor and a range-based sensor combination.

*Corresponding author: faizr@uthm.edu.my

Visual sensors or cameras rely on capturing the images of the environment and objects to give useful information to be extracted. The benefits of using cameras are their small size, lesser weight, lower power consumption, flexibility and they can be easily mounted. The operation of a light detection and ranging (LiDAR) sensor is remarkably similar to a radar. The LiDAR method of data collection is both quick and precise. Furthermore, compared to previous generations, LiDAR sensors have gotten significantly smaller, compact, and lighter in weight over time, and are now suitable for placement on small and micro-UAVs. The proposed obstacle detection system is projected to outperform the previously developed obstacle detection and avoidance system for UAV by combining these sensors into a single system.

The objective for this project is to construct an obstacle detection system by categorizing feature points identified in the image frames. Because of the previous obstacle detection system limitation which mainly focus on detecting obstacles that are directly in front of the UAV, this project also aims investigate the proposed method for the detection of free region toward both single and multiple obstacles with different physical configurations.

2. Methodology

This section presents the research methodology that is employed in the proposed obstacle detection system.

2.1 Proposed Project Configuration

The suggested obstacle detection system combines various sensors into a single detection system. Adding a sensor to the detecting system will modify the physical configuration of the UAV platform as well as the system's complexity. The UAV platform chosen in this work is the F450 quadcopter drone. Fig. 1 illustrates the configuration of the F450 quadcopter drone used in the research project and the frame work of the proposed obstacle detection system.

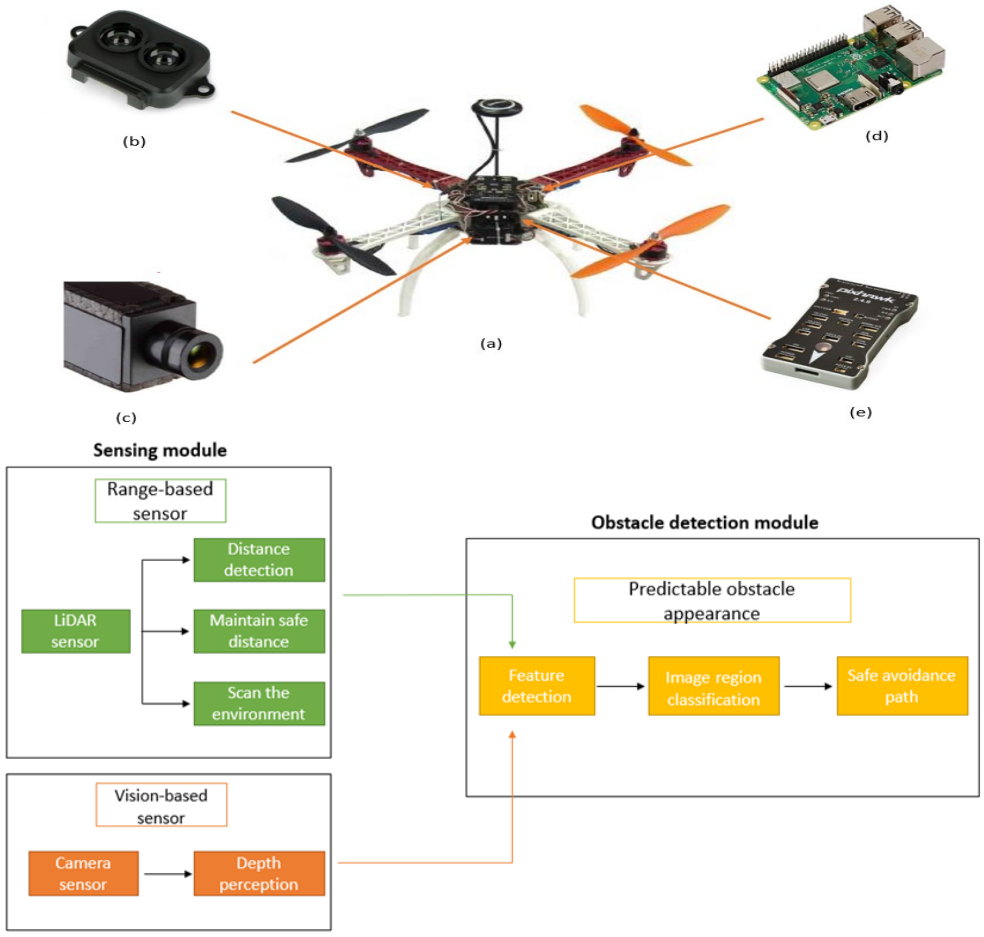

(f)

Fig. 1 - UAV platform configuration. (a) F450 quadcopter drone; (b) TF-Luna Lidar sensor; (c) camera sensor; (d) Raspberry Pi; (e) Pixhawk; (f) flow chart of the proposed obstacle detection system

The complementary sensor that will be used together with the camera sensor is the TF-Luna LIDAR. The TF-Luna is a ToF-based single-point ranging Lidar. It can provide consistent, accurate and very sensitive range measuring thanks to its unique optical and electrical design. Aside from that, the detection range of the TF-Luna is up to 8 metres, the blind zone is 0.2 metres and the distance resolution is 1 cm. With a standard deviation of 90 percent reflectivity, TF-Luna can detect objects with a minimum edge length of 3.5 cm within a detection distance of 1 metre. The TF-Luna's power supply voltage is 5V with a UART communication interface and a 3.3V communication level. Furthermore, TF-Luna is a little device that weighs about 5 grammes making the TF-Luna Lidar is an excellent choice and suitable solution for lightweight UAV applications. It is also compatible with Arduino, Raspberry Pi and other platforms.

2.2 ORB Features Detection and Binary Descriptor

ORB stands for Oriented Fast and Rotated Brief. The keypoints detector of ORB is FAST while the descriptor is BRIEF. To detect feature points, the ORB method employs the improved FAST (features from accelerated segment test) algorithm. The concept is that if a pixel differs greatly from its surroundings, it is more likely to be a corner point. After extracting the Oriented FAST feature points, the ORB method calculates the descriptors for each point using the enhanced BRIEF algorithm. BRIEF is a binary vector descriptor with a number of 0 and 1 values in its vector [8]. The image matching flow based on ORB algorithm and the example of features detection using ORB are shown in the Fig. 2 and Fig. 3 respectively.

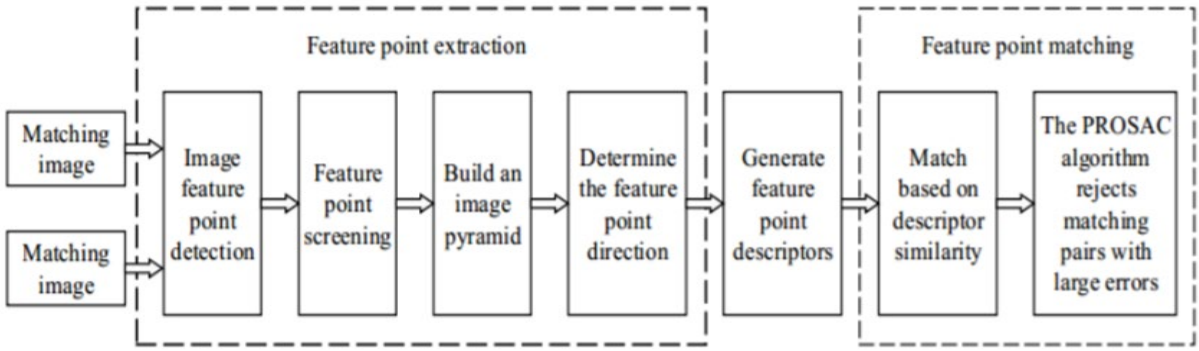

Fig. 2 - Image matching flow chart based on ORB algorithm [3]

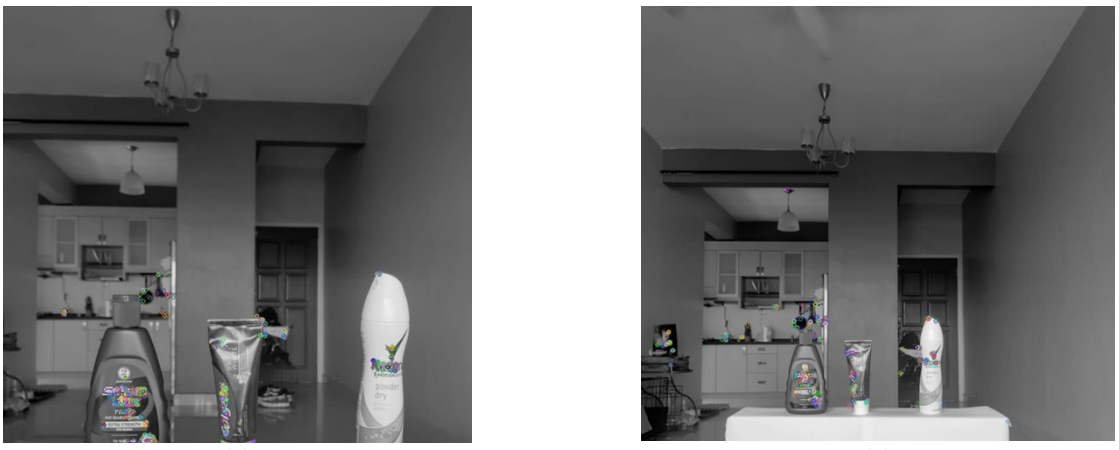

(a) **(b)**

Fig. 3 - Features detection using ORB algorithm (a) query image; (b) train image

2.3 Key Point Matching

ORB is a fusion of the FAST key point detector and BRIEF descriptor with some modifications [9]. Initially, it uses FAST to determine the main points. Then, the top N points are then determined using the Harris corner measure. FAST is rotation variant and does not compute the orientation. It calculates the patch's intensity weighted centroid with the corner in the centre. The orientation is determined by the direction of the vector from this corner point to the centroid. To increase rotation invariance, moments are computed. If there is an in-plane rotation, the descriptor BRIEF performs poorly. In ORB, the orientation of the patch is used to build a rotation matrix and then the BRIEF descriptors are steered accordingly. The example of keypoints matching across two image frames is shown in the Fig. 4.

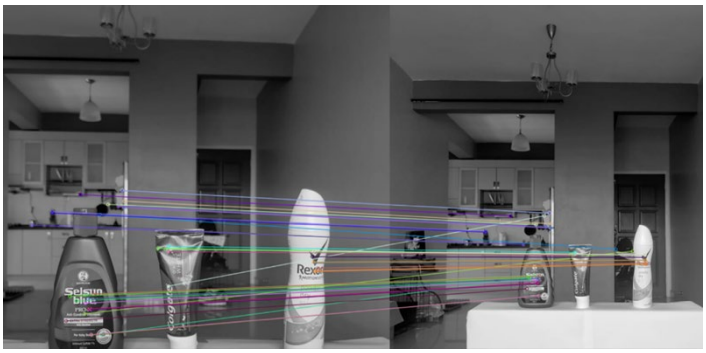

Fig. 4 - The matching key points across two image frames

2.4 Depth Perception Technique

The depth perception technique used by the proposed obstacle detection and avoidance system is based on the expansion of the detected features points between the image frames [10], [11]. This technique allows the suggested obstacle detection and avoidance system to simultaneously detect the existence of dangerous obstacles as well as free regions from the surrounding environment. The distance ratio cue and the octave scale change cue are two types of depth cues by expansion employed in the proposed obstacle detection and avoidance system. For the proposed UAV detection system, the distance ratio cue will be the major source, while the octave scale changes cue will be the secondary source.

2.4.1 Distance Ratio Cue Experiment

The main purpose of this experiment is to determine the distance ratio of the feature points across the image frames. Each of the image frames corresponds to the distance of the camera sensor to the target object [12] The image frames of the target object are captured in 10 cm increments until 300 cm is reached. As illustrated in Fig. 5(a), the target object has four feature points with four sets of distance values and it will be applied to all image frames. The four sets of distances from the feature points have comparable behavior as shown in Fig 5(b). It is also important to note that the distance between feature points and the camera sensor is inversely proportional to each other, closely resembling a logarithmic function. This result of this experiment can provide useful information, such as the fact that a closer object will have more substantial distance variations between feature points than an object at a distance. This information was used to discriminate between close and far objects in the surrounding environment. The suggested obstacle detection and avoidance system, on the other hand, would use this information to assist in recognizing the existence of obstacles in the UAV operating environment and, eventually, identify the best path for the UAV to take for a safe avoidance maneuver.

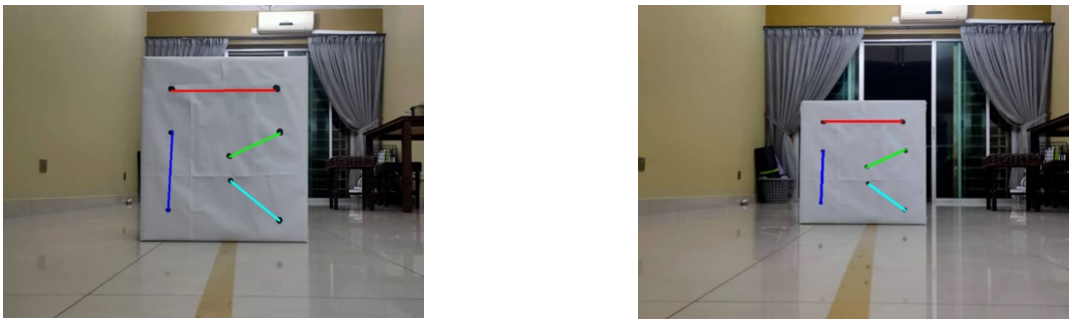

(a)

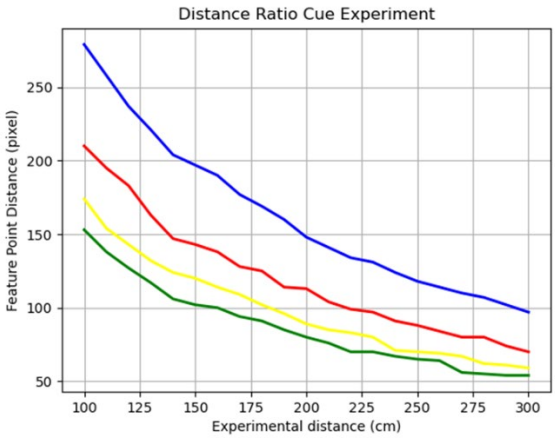

(b)

Fig. 5 - Distance feature point experiment (a) set of feature points distance; (b) distance ratio cue result (blue line is SOP 1, red line is SOP 2, yellow line is SOP 3, green line is SOP 4)

From the raw data collected, the distance ratio between corresponding feature point can be obtained. Table 1 shows the distance ratio with distance difference of 30cm.

Table 1 - dR for 30cm

Distance, cm	SOP 1	SOP 2	SOP 3	SOP 4	dR1	dR2	dR3	dR4	Average dR
100	210.1	279.1	153.5	173.5	1.29	1.26	1.31	1.32	1.30
110	195.1	258.0	138.2	154.2	1.33	1.26	1.30	1.24	1.28
120	183.3	237.0	127.0	142.0	1.17	1.17	1.24	1.18	1.16
130	163.0	221.0	117.2	131.6	1.16	1.16	1.17	1.16	1.16
140	147.2	204.0	106.9	124.3	1.15	1.15	1.14	1.14	1.15
150	142.2	203.0	102.1	120.2	1.14	1.13	1.12	1.11	1.13
160	140.1	190.0	100.3	113.7	1.13	1.12	1.11	1.10	1.12

From the table above, the recommended reference distance ratio would be 1.13 as the proposed obstacle detection system is designed to execute the algorithm when approaching the obstacle at 150cm. The observed reference points will be thresholded using a straightforward technique. If the distance ratio is greater than the reference distance ratio, the detecting system will identify the matching feature points as an obstacle meanwhile if the distance ratio is smaller than the reference distance ratio, the matching feature will be considered as non-obstacle.

2.4.2 Octave Scale Change Experiment

The scale changes cue is provided with the distance ratio cue to add reliability to the proposed obstacle identification and avoidance system. These scale values will change depending on how far away the image frame was taken. When a similar feature point from an object is identified at a greater distance from the camera sensor for example, the scale value created is practically smaller in comparison to the scale value obtained when the camera sensor is extremely close to the object. As a result, changes in the scale values of identified feature points might provide imprecise information on the object's state position, which is either approaching or moving away from the UAV.

Two set of image frame were taken from the same camera as shown in the Fig. 6. The first image is taken 170cm from the camera, while the second image frame is taken 200cm from the camera. Theoretically, when a similar feature point from an object is detected at a wider sensor is extremely distance from the camera sensor, the octave scale value generated is essentially less than when the camera close to the object. The total value of the octave scale can be the parameter to filter out the false matching. Referring to the Table 2 below, it can be concluded that the keypoint with index number 14 is not a true keypoint as its scale value in image frame 2 is higher than in image frame 1, thus it can be executed from the detection algorithm.

(a) **(b)**

Fig. 6 - Scale change experiment (a) image frame 1 (170cm); (b) image frame 2 (200cm)

Table 2 - Octave scale difference between two images

Index	Octave value image 1,	Octave value image 2,	Total octave value	Status
9	3	2	1	True
10	0	0	0	True
11	1	1	1	True
12	2	2	0	True
13	2	2	0	True
14	5	6	-1	False
15	5	4	1	True

3. Result and Discussion

This section discusses the findings of the proposed obstacles detection algorithm.

3.1 Single Frontal Obstacle

There are three types of obstacles introduced inside the operating environment. The obstacles are varied due to the intensity of the texture and size of the obstacles. The first type is the obstacle with heavy texture, the second type is obstacle with semi or moderate texture and the last type would be the obstacle with texture-less character. The objective of this experiment is to evaluate the effectiveness of the proposed obstacle detection system, particularly when dealing with frontal obstructions that can have a range of physical configurations. The image frames are captured when the camera approaching the obstacles at the distance 150cm and 120cm as shown in the Fig. 7.

As shown in the Fig. 8, there are two different colours of circles pointed randomly in the result images. Note that the red circles indicate the feature points that can considered as potential obstacles while the blue circles indicate as free regions. Generally, the proposed algorithm successfully differentiates the potential obstacles and the free region but it still can be observed that after using the ratio cue expansion and the thresholding the distance ratio, there still few key-points that can be classified as false key-points. Despite of the imperfection of the proposed obstacles detection algorithm, it still provided a reliable result as high intensity of the blue circles are mostly located at the background of the image and not within the obstacles.

The suggested algorithm may only be deemed effective if the percentage of true key points is more than the percentage of false key points or to put it another way, if the percentage of true key points is in theory should be greater than 50%. Calculating the presumption percentage of the true key-points will be simpler once the percentage of false key-points has been identified. The percentages of the true keypoints for single frontal obstacles are shown in the Table 3.

Fig. 7 - Captured image of the texture-less obstacle at (a) 150 cm; (b) 120 cm, semi texture obstacle at; (c) 150 cm; (d) 120 cm, texture-less obstacle at; (e) 150 cm; (f) 120cm

Table 3 - The percentage of true keypoints for single obstacle

Type of obstacles	Total number of circles		Assumption number of false circles		Percentage of true key-points (%)	
	Blue	Red	Blue	Red	Blue	Red
Heavy texture	498	26	154	7	69.1	73.1
Semi texture	852	84	122	10	85.7	88.1
Texture-less	622	121	125	21	79.9	82.6

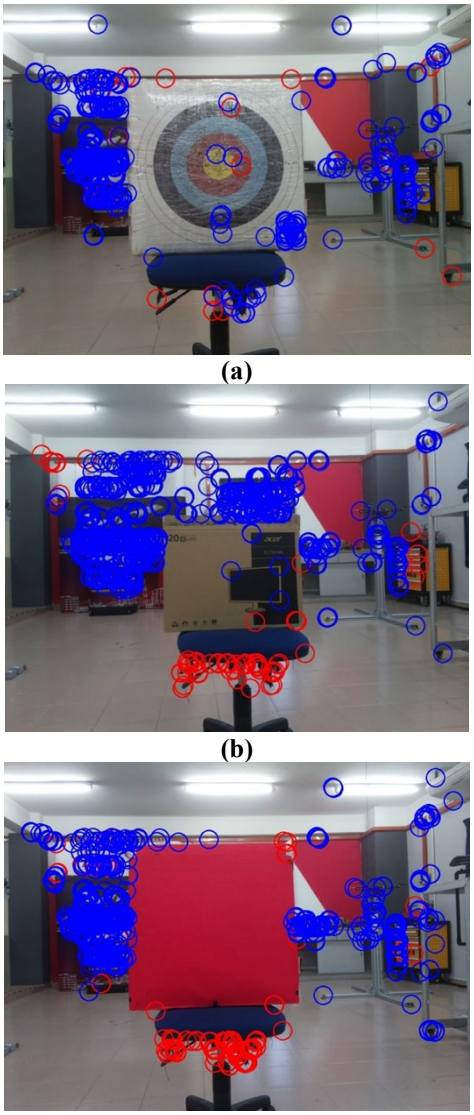

(a)

(b)

(c)

Fig. 8 - Result of the proposed algorithm on (a) heavy textures obstacle; (b) semi texture obstacle; (c) texture-less obstacle

3.2 Multiple Obstacles

In this situation, the frontal obstacle is joined by the side obstacle in the working environment depending on where the side obstacles are located, there are three different scenarios in the experiments. The front obstacle and the side obstacle in the first scenario must be completely aligned or at roughly the same distance from the camera. In contrast, in the second scenario, the frontal obstacle's position is maintained and the side obstacle is positioned 30 cm away from the frontal obstacle. In the third scenario, the obstacle's position is constant but the side obstacle's distance from the frontal obstacle is raised by 50 cm. The experiments are conducted on both sides as each time the frontal obstacle's side obstacle is shifted from the right side to the left side.

3.2.1 Scenario 1: Side Obstacle Aligned to Frontal Obstacle

The result of the first scenario is shown in the Fig. 9 below. It is clearly can be observed that the high intensity of the blue circles is at the background of the images while the red circles mostly detected on the obstacles. Although the result seems reliable, it is undeniable that still have few false key-points detected. As can be observed in Fig.9(a), there are lot of red circles pointed at the background of the image while in the Fig. 9(b), the false red circles detected other on the obstacles are not much as when the side obstacle in in the left side. Thus, in order to evaluate the effectiveness of the proposed obstacle detection algorithm, the percentage of the true key-points need to be calculated as shown in the Table 4.

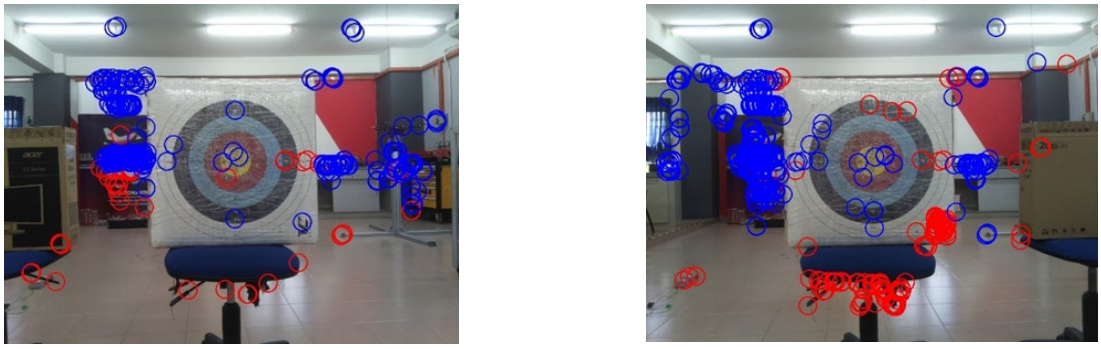

(a) (b)

Fig. 9 - Result for the aligned obstacles (a) left; (b) right

Table 4 - The percentage of true key points for scenario 1

Position of side obstacle	Total numbers of circles		Assumption number of false keypoints		Percentage of true key-points (%)	
	Blue	Red	Blue	Red	Blue	Red
Left	315	54	62	28	80.3	48.1
Right	458	150	77	44	83.2	70.7

3.2.2 Scenario 2: Side Obstacle 30cm Away from Frontal Obstacle

The result for the second scenario is shown in the Fig. 10. Compared to the result from the first scenario, an increment of 30cm of the side obstacles away from the frontal obstacle granted a more positive result. This is because the proposed algorithm managed to detect the side obstacle as a potential obstacle as well as frontal obstacle. The side obstacle is more visible in the image frame compared to when both of the obstacles are put aligned to each other thus make it to have higher chance to be detect as a potential obstacle. The result when the side obstacle at the right side seems to be more reliable as most of the blue circles are in the background and most of the red circles are detected on the obstacles. On the other hand, as can be observed from the result when the side obstacle is at the left side, there are many obvious false keypoints can be seen as the blue circles are detected on the frontal obstacles. The percentage of true keypoints for the second scenario is shown in the Table 5.

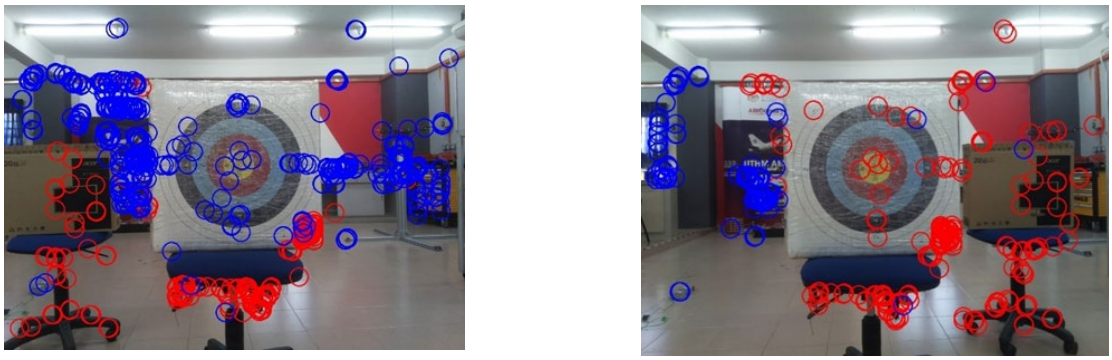

(a) (b)

Fig. 10 - Result for side obstacle 30cm away from frontal obstacle (a) left; (b) right

Table 5 - The percentage of true key points for scenario 2

Position of side obstacle	Total numbers of circles		Assumption number of false keypoints		Percentage of true key-points (%)	
	Blue	Red	Blue	Red	Blue	Red
Left	494	215	129	21	73.9	90.2
Right	126	205	23	25	81.7	87.8

3.2.3 Scenario 3: Side Obstacle 50cm Away from Frontal Obstacle

The result for the third scenario is shown in the Fig. 11. Compared to the result from the second scenario, when the side obstacle is positioned 50cm away from the frontal obstacles, the proposed obstacle detection algorithm executed ambiguous outcomes. As can be seen from the Fig. 11(a), the side obstacle has been considered as free region because the high intensity of blue circles is detected in the background of the image and also including the side obstacle. Meanwhile on the other hand, for the Fig. 11(b), the side obstacle is successfully detected as a potential obstacle but the right side of the background of the image also be detected as a potential obstacle as high intensity of red circles can be seen on that region. Undergo the same working environment and executed with the same proposed obstacles detection algorithm, the percentage of true keypoints also must be calculated similarly with the other scenarios. But in this scenario, only the true keypoints are calculated manually as there are redundant false keypoints detected in this scenario. The result is shown in the Table 6.

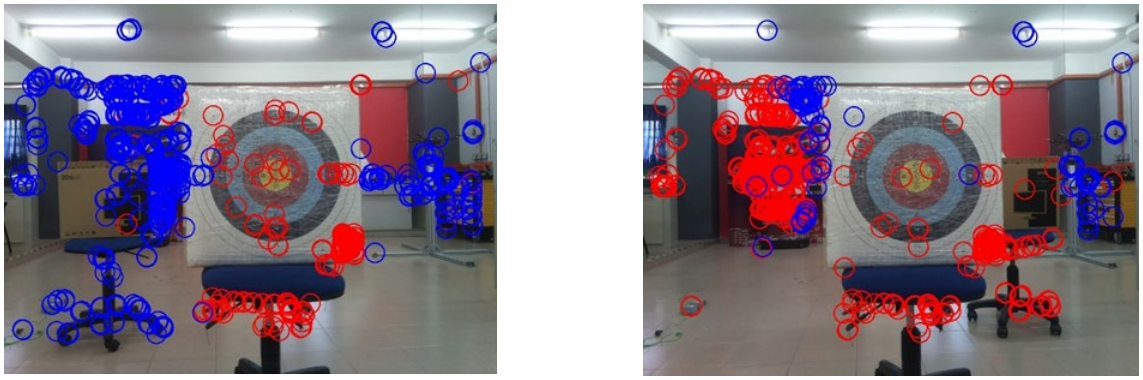

(a) **(b)**

Fig. 11 - Result for side obstacle 50cm away from frontal obstacle (a) left; (b) right

Table 6 - The percentage of true key points for scenario 3

Position of side obstacle	Total numbers of circles		Assumption number of false keypoints		Percentage of true key-points (%)	
	Blue	Red	Blue	Red	Blue	Red
Left	648	182	155	11	76.1	94.0
Right	122	624	27	282	77.9	54.8

4. Conclusion

This project presents the research work for the obstacle detection for the small UAVs. The main purpose of this research is to create a system for categorizing feature points identified in image frames so the obstacle detection system can create a safe avoidance path. By developing a revolutionary obstacle detection and avoidance system based on a vision-based sensor and a range-based sensor combination, this research seeks to outperformed all of the aforementioned faults and problems. The proposed obstacle detection and avoidance system is expected to perform better than the obstacle detection system for UAVs that was previously developed by integrating various sensors into a single system. Even after using depth perception technique, the proposed detection system may stand a chance to be a reliable system but that does not mean the proposed system is flawless. As can be observed from the result, the proposed algorithm system works perfectly to detect and differentiate between the potential obstacles and free region for a single frontal obstacle. The proposed detection system somehow detects the background of the image as potential obstacles even the distance of the camera from the background is distant.

Acknowledgement

This research was supported by Universiti Tun Hussein Onn Malaysia (UTHM) through Tier 1 Grant (H920).

References

[1] F. Kendoul, “Survey of Advances in Guidance, Navigation, and Control of Unmanned Rotorcraft Systems,” *J Field Robot*, vol. 29, no. 2, pp. 315–378, 2012, doi: 10.1002/rob.

[2] T. Merz and F. Kendoul, "Beyond visual range obstacle avoidance and infrastructure inspection by an autonomous helicopter," *IEEE International Conference on Intelligent Robots and Systems*, pp. 4953–4960, 2011, doi: 10.1109/IROS.2011.6048249.

[3] D. Erdos, A. Erdos, and S. E. Watkins, "An experimental UAV system for search and rescue challenge," *IEEE Aerospace and Electronic Systems Magazine*, vol. 28, no. 5, pp. 32–37, 2013, doi: 10.1109/MAES.2013.6516147.

[4] B. T. Tomi *et al.*, "Research Platform for Indoor and Outdoor Urban Search and Rescue," *Robotics and Automation Magazine*, 2012.

[5] J. Scherer *et al.*, "An Autonomous Multi-UAV System for Search and Rescue," *Proceedings of the First Workshop on Micro Aerial Vehicle Networks, Systems, and Applications for Civilian Use - DroNet '15*, pp. 33–38, 2015, doi: 10.1145/2750675.2750683.

[6] P. Rudol and P. Doherty, "Human Body Detection and Geolocalization for UAV Search and Rescue Missions Using Color and Thermal Imagery .," in *IEEE aerospace conference*, 2008, pp. 1–8.

[7] C. Eschmann, C.-M. Kuo, and C. Boller, "Unmanned Aircraft Systems for Remote Building Inspection and Monitoring," *Proceedings of the 6th European Workshop on Structural Health Monitoring*, vol. 2, pp. 1–8, 2012.

[8] E. Rublee, V. Rabaud, K. Konolige, and G. Bradski, "ORB: An efficient alternative to SIFT or SURF," *Proceedings of the IEEE International Conference on Computer Vision*, pp. 2564–2571, 2011, doi: 10.1109/ICCV.2011.6126544.

[9] E. Karami, S. Prasad, and M. Shehata, "Image Matching Using SIFT, SURF, BRIEF and ORB: Performance Comparison for Distorted Images," *ArXiv*, 2017.

[10] M. F. Ramli and S. S. Shamsudin, "Obstacle detection technique to solve poor texture appearance of the obstacle by categorising image's region using cues from expansion of feature points for small UAV," *Int J Comput Vis Robot*, vol. 13, no. 1, pp. 91–115, 2022, doi: 10.1504/ijcvr.2022.10044362.

[11] M. F. Bin Ramli, S. S. Shamsudin, and A. Legowo, "Obstacle detection technique using multi sensor integration for small unmanned aerial vehicle," *Indonesian Journal of Electrical Engineering and Computer Science*, vol. 8, no. 2, pp. 441–449, 2017, doi: 10.11591/ijeecs.v8.i2.pp441-449.

[12] M. Faiz, B. Ramli, and A. Legowo, "Safe avoidance path detection using multi sensor integration for small Unmanned Aerial Vehicle".